

~~SECRET~~Copy
RM L50C22

3 1176 00039 9973

~~SECRET~~
NACA

~~404~~
Bell
X-1
Copy 2

RESEARCH MEMORANDUM

AERODYNAMIC AND LATERAL-CONTROL CHARACTERISTICS
OF A $\frac{1}{28}$ -SCALE MODEL OF
THE BELL X-1 AIRPLANE WING-FUSELAGE COMBINATION

TRANSONIC-BUMP METHOD

By Vernard E. Lockwood

CLASSIFICATION CHANGED TO ~~CONFIDENTIAL~~
Langley Aeronautical Laboratory
Langley Air Force Base, Va.

~~CONFIDENTIAL~~

CLASSIFICATION CANCELLED

Authority *NACA Reauth. 710-511* Date *May 15, 1981*

By *DeGard* See *May 25, 1981*

Authority *NACA R 7-2521* Date *8/23/54*

2424 9/7/54 See

NATIONAL ADVISORY COMMITTEE
FOR AERONAUTICS

WASHINGTON

May 5, 1950

UNCLASSIFIED

~~SECRET~~~~CONFIDENTIAL~~

NACA LIBRARY

LANGLEY AERONAUTICAL LABORATORY
Langley Field, Va.

ERRATUM

File X-1/3

NACA RM L50C22

AERODYNAMIC AND LATERAL-CONTROL CHARACTERISTICS OF A $\frac{1}{28}$ -SCALE MODEL OF

THE BELL X-1 AIRPLANE WING-FUSELAGE COMBINATION

TRANSONIC-BUMP METHOD
By Vernard E. Lockwood

May 5, 1950

Figure 14: An error in the curve for Model $C_L = 0.4$ has been corrected in the figure below, which should replace figure 14 in the published copy of this paper. This revision in no way affects the results or conclusions presented.

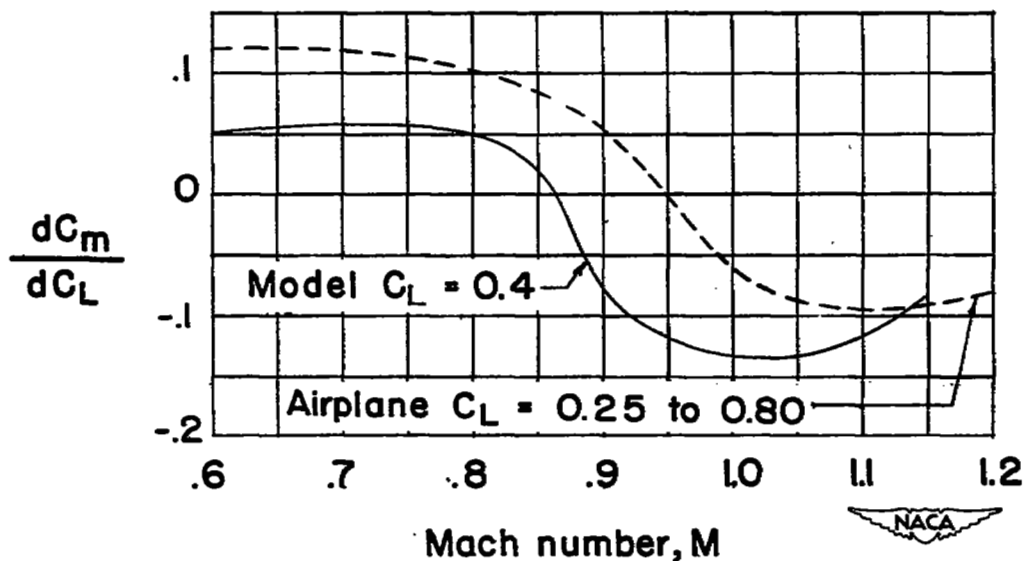


Figure 14 - Comparison of $\frac{dC_m}{dC_L}$ obtained between model and airplane. Center of gravity at .236 MAC.

~~CONFIDENTIAL~~ UNCLASSIFIED

NATIONAL ADVISORY COMMITTEE FOR AERONAUTICS

RESEARCH MEMORANDUM

AERODYNAMIC AND LATERAL-CONTROL CHARACTERISTICS

OF A $\frac{1}{28}$ - SCALE MODEL OF

THE BELL X-1 AIRPLANE WING-FUSELAGE COMBINATION

TRANSONIC-BUMP METHOD

By Vernard E. Lockwood

SUMMARY

An investigation was made to determine the lateral-control characteristics and the pitching-moment characteristics of a $\frac{1}{28}$ - scale model of the X-1 wing-fuselage configuration. The tests were made in the transonic speed range from a Mach number of 0.60 to 1.15 in the Langley high-speed 7- by 10-foot tunnel utilizing the transonic bump. Comparisons are included between available flight data and wind-tunnel results.

The results of the lateral-control investigation showed that the rolling effectiveness varied with Mach number in a manner similar to the flight-test results at Mach numbers between 0.6 and 1.06. There were differences, however, in the absolute values which might be accounted for in part by the gap conditions at the nose of the aileron; the aileron of the model is sealed, whereas that of the airplane is unsealed. The measured slopes of the pitching-moment curves of the model also varied with Mach number in a manner similar to that obtained on the airplane. There were differences in the absolute values of the slopes but the data from the model were not directly comparable with the data from the airplane.

INTRODUCTION

An investigation was made at transonic speeds to determine the lateral-control and pitching-moment characteristics of a $\frac{1}{28}$ - scale model

SECRET

~~CONFIDENTIAL~~

UNCLASSIFIED

of the X-1 wing-fuselage combination using the transonic-bump technique. The investigation was made for the purpose of correlating with flight data. In the investigation the aileron effectiveness, damping in roll, lift, pitching moments, and wing bending moments of the model were determined.

Two similar wing models were used in the investigation, having an aspect ratio of 6.0, taper ratio 0.5, and an unswept 40-percent-chord line. The wings had NACA 65-108 airfoil sections and a twist distribution corresponding to 1° of washout. One wing was constructed with a 15-percent-chord aileron and the other, with an additional twist with linear variation from root to tip corresponding to 4.72° of washin at the tip. Damping-in-roll characteristics were obtained on the assumption that the damping moment of a rolling wing would be equal to the rolling moment produced by the addition of linear twist along the span.

The aileron rolling effectiveness has been calculated and a comparison with flight data is given up to a Mach number of 1.06. Comparisons of the pitching-moment characteristics and lateral centers of pressure with flight data are also included.

COEFFICIENTS AND SYMBOLS

C_L	lift coefficient (Twice lift of semispan model/ qS)
C_m	pitching-moment coefficient referred to $0.25\bar{c}$ (Twice pitching moment of semispan model/ $qS\bar{c}$)
C_B	bending-moment coefficient about root-chord line at plane of symmetry $\left(\text{Root bending moment}/q\frac{S}{2}\frac{b}{2}\right)$
C_l	rolling-moment coefficient about root-chord line at plane of symmetry (Rolling moment/ qSb)
C_{l_a}	increment in rolling-moment coefficient caused by deflection of aileron at a given angle of attack $(C_{l_{\text{aileron deflected}}} - C_{l_{\text{aileron undeflected}}})$
C_{l_p}	damping-in-roll coefficient $\left(-2(C_{l_{\text{twisted wing}}} - C_{l_{\text{untwisted wing}}})\frac{2v}{pb}\right)$
S	twice wing area of semispan model, 0.165 square foot

b	twice span of semispan model, 1.000 foot
b'	twice span of wing outside of fuselage
\bar{c}	mean aerodynamic chord of wing, 0.171 foot; based on relationship $\frac{1}{S} \int_0^{b/2} c^2 dy$ (using theoretical tip)
c	local wing chord
y	spanwise distance from plane of symmetry
y'	spanwise distance from fuselage
q	effective dynamic pressure over span of model, pounds per square foot $\left(\frac{1}{2}\rho V^2\right)$
ρ	air density, slug per cubic foot
V	free-stream velocity, feet per second
M	effective Mach number over span of model
M_l	local Mach number
M_a	average chordwise local Mach number
R	Reynolds number of wing based on \bar{c}
α	angle of attack, referred to wing root-chord line, degrees
δ_a	aileron deflection, positive when trailing edge is down, degrees
$\phi_{b/2V}$	wing-tip helix angle, radians
p	rate of roll corresponding to a given airspeed, radians per second

MODEL AND APPARATUS

The investigation was performed on a $\frac{1}{28}$ -scale semispan model of the X-1 airplane wing-fuselage combination. In this investigation two

wing models were used, one to obtain the aerodynamic characteristics in pitch and the aileron effectiveness, and the other, to determine the damping-in-roll coefficient. The details of the basic wing-fuselage combination are shown in figure 1.

The aileron of the control model was simulated by cutting the steel wing at the proper spanwise stations from trailing edge to aileron hinge line (85-percent-chord line) and cutting grooves of $\frac{1}{32}$ -inch width along the hinge line on both the upper and lower surfaces of the wing as is shown in the typical section of figure 1. The desired aileron deflection was obtained by bending at the aileron hinge line. The grooves were faired over with wax to eliminate breaks in the airfoil contours, thus simulating a plain sealed aileron.

The damping-in-roll wing was twisted so as to provide an additional angle-of-attack distribution which varied linearly along the span of the model. The measured twist is shown in figure 2 and corresponds to 4.72° of washin at the tip. (It should be noted that the basic model had 1° of washout.)

The half fuselage used in the investigation was made of brass and was bent to conform to the bump contour as shown in figure 1. The wings were interchangeable on this fuselage. The ordinates of the fuselage, which is a cylinder of revolution, are given in table I.

A five-component balance of the strain-gage type was installed beneath the surface of the bump and measured forces and moments with respect to the wind axes.

TESTS

The models were tested in the Langley high-speed 7- by 10-foot tunnel utilizing the flow field over the transonic bump to obtain Mach numbers from 0.6 to 1.15. Typical contours of local Mach number in the vicinity of the model location on the bump are shown in figure 3. It is seen that there was a Mach number variation of about 0.08 over the model semispan at low Mach numbers and about 0.12 at the highest test Mach numbers. The chordwise Mach number variation was generally less than 0.02. No attempt has been made to evaluate the effects of this chordwise and spanwise Mach number variation. The effective test Mach number was obtained from contour charts similar to those presented in figure 3 using the relationship

$$M = \frac{2}{S} \int_0^{b/2} cM_a dy$$

The variation of mean Reynolds number with test Mach number is shown in figure 4. The boundaries in the figure are an indication of the probable range in Reynolds number caused by variations in atmospheric conditions in the course of the investigation.

Reflection-plane correction factors, which account for the carry-over of load to the other wing, have been applied to the aileron data and the damping-in-roll data. The correction factors, which are 0.87 for the aileron data and 0.89 for damping-in-roll data, were determined by using span loadings obtained from reference 1. The variation of these correction factors with Mach number is not known but it is thought that the correction approaches zero at a Mach number of 1.0. The error caused by neglecting the effects of Mach number on the reflection-plane corrections, however, is alleviated somewhat if the damping-in-roll and aileron-effectiveness data are used in conjunction with each other.

The tests were conducted at constant values of α and δ_a from a Mach number of 0.60 to 1.15. Aileron deflections of 0° , $\pm 6^\circ$, and $\pm 12^\circ$ were investigated. The angle of attack was varied from 0° to 10° in 2° increments.

RESULTS AND DISCUSSION

The results of the investigation are presented in the following figures:

	Figures
Aerodynamic characteristics in pitch	5
Aileron characteristics	6, 7
Damping-in-roll characteristics	8, 9, 10
Estimated rolling effectiveness :	11
Summary data:	
Lift-curve slopes	12
Pitching-moment characteristics	13, 14, 15
Lateral centers of pressure	16

Lateral-Control Characteristics

The summary of aileron characteristics (fig. 7) shows that the aileron effectiveness was considerably affected by angle of attack and Mach number. The aileron effectiveness generally decreased with Mach number above $M = 0.8$; however, the effects were more pronounced at the lower angles of attack than at the higher angles. For example, a large loss in effectiveness occurred between $M = 0.90$ and $M = 0.95$

for $\alpha = 2^\circ$, whereas at $\alpha = 6^\circ$ the loss was small in comparison. These characteristics result in showing increasing values of $C_{l\delta_a}$ with increase of α at $M = 0.92$ or above, whereas at lower Mach numbers, $C_{l\delta_a}$ decreases with angle of attack.

The aileron effectiveness obtained agrees fairly well with low-speed data on the X-1 10-percent-thick wing (unpublished data) as shown in figure 7.

In addition to the aileron effectiveness $C_{l\delta_a}$, the damping-in-roll coefficient of a wing C_{lp} must be known before estimations can be made of the airplane rate of roll. The difference in rolling moments of the untwisted wing and the twisted wing, of which figure 8 is typical, is a measure of the damping. The assumption is made that the damping moment of a steady rolling wing will be equal to the rolling moment resulting from a linear variation of twist along the span. The damping-moment coefficient in roll is therefore:

$$C_{lp} = -2\left(\frac{2V}{pb}\right)(0.87)(C_{l_{\text{twisted}}} - C_{l_{\text{untwisted}}})$$

where the additional wing twist represents a $pb/2V$ of 0.0825 radians and 0.87 is the reflection-plane correction factor.

A comparison of the theoretical values of C_{lp} obtained from reference 2 with the experimental results shows good agreement up to $M = 0.85$, figure 9. The damping in roll remained fairly high throughout the Mach number range and, as might be expected, varied in a manner similar to lift-curve slope. The similarity is apparent in figure 10 where the ratio of C_{l_α} or C_{lp} at any Mach number to its respective value at a Mach number of 0.6 is given.

An estimation of the rolling effectiveness of the aileron-wing configuration is given in figure 11 using the aileron effectiveness and damping in roll experimentally determined. A comparison is also given with the flight results from references 3 and 4 up to a Mach number of 1.06. The flight data are on a 10-percent-thick wing. The estimated values of $\frac{pb}{2V}/\delta_a$ are greater than the flight values but the variation of $\frac{pb}{2V}/\delta_a$ with M is similar.

~~CONFIDENTIAL~~

A considerable part of the difference in the values of $\frac{pb}{2V} \delta_a$ obtained on the model and the airplane may be the result of the gap conditions at the nose of the aileron. The aileron of the airplane is unsealed, whereas the model aileron is effectively sealed. From previous investigations at low Mach numbers it is known that an unsealed aileron gives less effectiveness than a sealed aileron. Reference 5 shows that an aileron of corresponding size would be only 65 percent as effective as a sealed aileron. If this factor were applied to the wind-tunnel data, the agreement with flight data would then be relatively good at subsonic Mach numbers. There is also evidence, reference 6, that a difference in effectiveness exists at supercritical Mach numbers, although these data are for a swept wing with a circular-arc airfoil section.

A small part of the difference in $\frac{pb}{2V} \delta_a$ between flight and wind-tunnel data may also be attributed to wing flexure, and a minor part, to aileron contour. Aileron deflection causes a torsional moment that tends to twist the wing, resulting in reduced rolling effectiveness. The airplane wing would twist more than the very rigid, solid, steel wing. It has been estimated from reference 7 that a reduction factor of $3\frac{1}{2}$ percent should be applied to the tunnel data at $M = 0.80$ for correspondence with flight conditions. The model has a true contour aileron with a cusp and may have had slightly greater effectiveness than the flat-sided aileron on the airplane.

Aerodynamic Characteristics in Pitch

The lift-curve slopes obtained from the data of the present investigation, figure 5, are compared with those obtained from other sources in figure 12. The agreement of lift-curve slopes obtained between the model of the present investigation and some unpublished data on a $\frac{1}{40}$ -scale bump model is excellent. In the subsonic speed range the experimental lift-curve slopes also agreed very well with theoretical slopes obtained from reference 2. A point from an investigation of a $\frac{1}{14}$ -scale model (10-percent-thick wing) at $M = 0.35$ (unpublished data) is included in figure 12 for comparison.

The variation of dC_m/dC_L with Mach number shown in figure 13 for the model wing-fuselage combination is large and irregular, especially at low lift coefficients. The data, which are for a center-of-gravity location of 25 percent mean aerodynamic chord, show a rearward shift of the aerodynamic center from 15 to 20 percent of the mean aerodynamic

~~CONFIDENTIAL~~

chord between Mach numbers of 0.60 to 1.05. A forward shift of the aerodynamic center occurs between a Mach number of 0.85 and 0.88 for a $C_L = 0$. At lift coefficients in the normal operating range of the airplane ($C_L = 0.20$ or above) the tendency for the forward shift is not evident.

A comparison of dC_m/dC_L from the present investigation with the results of unpublished flight tests at the NACA High-Speed Flight Research Station at Edwards Air Force Base, Calif., on the 8-percent-thick wing is presented in figure 14. These data show that the variation of dC_m/dC_L with Mach number from the model was similar to that obtained with the airplane. There was, however, a considerable difference in absolute magnitude of dC_m/dC_L between model and airplane. The results are not directly comparable because the flight data are given for a lift coefficient which varies from values of 0.25 to 0.80, whereas the wind-tunnel data are for a lift coefficient of 0.40. Part of the difference in dC_m/dC_L may be attributed to experimental accuracy. The probable accuracy of dC_m/dC_L for the wind-tunnel data is ± 0.02 . The accuracy of the flight data appears to be less, particularly near a Mach number of 0.9 where there is a large scatter in the data.

A comparison of the tail-off pitching-moment coefficients is given in figure 15 between the model of the present investigation and the flight results on the 8-percent-thick wing, reference 8. The tail-off pitching-moment coefficients of the airplane were calculated from the horizontal-tail loads measured in flight for a center of gravity which varied from 22.1 to 25.3 mean aerodynamic chord. The pivot point of the model was at 25 percent mean aerodynamic chord. The model results are in good agreement with flight results as to the variation of pitching-moment coefficients with Mach number, but the values of C_m for the wind-tunnel data are considerably more negative. Part of the difference might be attributed to the pitching moments caused by the drag of the empennage.

The lateral center of pressure of the wing-fuselage combination remained fairly close to the 40-percent-span station throughout the Mach number range tested as is shown in figure 16. Unpublished data from flight tests at the NACA High-Speed Flight Research Station at Edwards Air Force Base, Calif., gave a lateral center of pressure of 42 percent span for the airplane based on the wing outside of the fuselage in contrast to the model data which are given about the wing center line. The airplane data were determined from strain gages mounted on the wing near the wing-fuselage juncture.

CONCLUSIONS

The results of wind-tunnel tests of a $\frac{1}{28}$ -scale model of the X-1 airplane to determine the lateral-control characteristics and the aerodynamic characteristics in pitch of the wing-fuselage configuration at transonic speeds indicated the following conclusions:

1. The estimated variation of rolling effectiveness with Mach number was similar to that achieved in flight on a 10-percent-thick wing, although the flight data showed lower effectiveness. A considerable part of the difference might be caused by the gap conditions at the nose of the aileron; the aileron of the model is sealed, whereas that of the airplane is unsealed. A large loss of aileron effectiveness, which was most pronounced for a low angle of attack, occurred between Mach numbers of 0.90 and 0.95. At subsonic Mach numbers the damping in roll obtained experimentally was in good agreement with theoretical results. The damping coefficient showed a variation with Mach number similar to that obtained with the lift-curve slope.

2. The slopes of the wing-fuselage pitching-moment-coefficient curves varied with Mach number in a manner similar to that obtained on the airplane. There were differences in the values of the slopes but the data were not directly comparable because the actual value of the airplane lift coefficients were unknown.

Langley Aeronautical Laboratory
National Advisory Committee for Aeronautics
Langley Air Force Base, Va.

REFERENCES

1. Pearson, Henry A., and Jones, Robert T.: Theoretical Stability and Control Characteristics of Wings with Various Amounts of Taper and Twist. NACA Rep. 635, 1938.
2. Polhamus, Edward C.: A Simple Method of Estimating the Subsonic Lift and Damping in Roll of Sweptback Wings. NACA TN 1862, 1949.
3. Drake, Hubert M.: Measurements of Aileron Effectiveness of Bell X-1 Airplane up to a Mach Number of 0.82. NACA RM L9D13, 1949.
4. Drake, Hubert M.: Measurements of Aileron Effectiveness of the Bell X-1 Airplane at Mach Numbers between 0.9 and 1.06. NACA RM L9G19a, 1949.
5. Weick, Fred E., and Jones, Robert T.: Résumé and Analysis of N.A.C.A. Lateral Control Research. NACA Rep. 605, 1937.
6. Turner, Thomas R., Lockwood, Vernard E., and Vogler, Raymond D.: Preliminary Investigation of Various Ailerons on a 42° Sweptback Wing for Lateral Control at Transonic Speeds. NACA RM L8D21, 1948.
7. Pearson, Henry A., and Aiken, William S., Jr.: Charts for the Determination of Wing Torsional Stiffness Required for Specified Rolling Characteristics or Aileron Reversal Speed. NACA Rep. 799, 1944.
8. Drake, Hubert M., McLaughlin, Milton D., and Goodman, Harold R.: Results Obtained during Accelerated Transonic Tests of the Bell XS-1 Airplane in Flights to a Mach Number of 0.92. NACA RM L8A05a, 1948.

TABLE I

FUSELAGE ORDINATES

X	Y
0.0	0.0
.357	.182
.714	.337
1.071	.471
1.429	.585
1.786	.683
2.143	.765
2.500	.833
2.857	.888
3.214	.929
3.571	.959
3.929	.976
4.286	.982
5.357	.982
5.714	.981
6.071	.978
6.429	.973
6.786	.965
7.143	.954
7.500	.940
7.857	.922
8.214	.900
8.571	.875
8.929	.847
9.286	.807
9.643	.782
10.000	.746
10.357	.704
10.714	.658
11.071	.609
11.429	.557
11.786	.502
12.143	.445
12.500	.386
12.857	.325
13.214	.263
13.286	.250

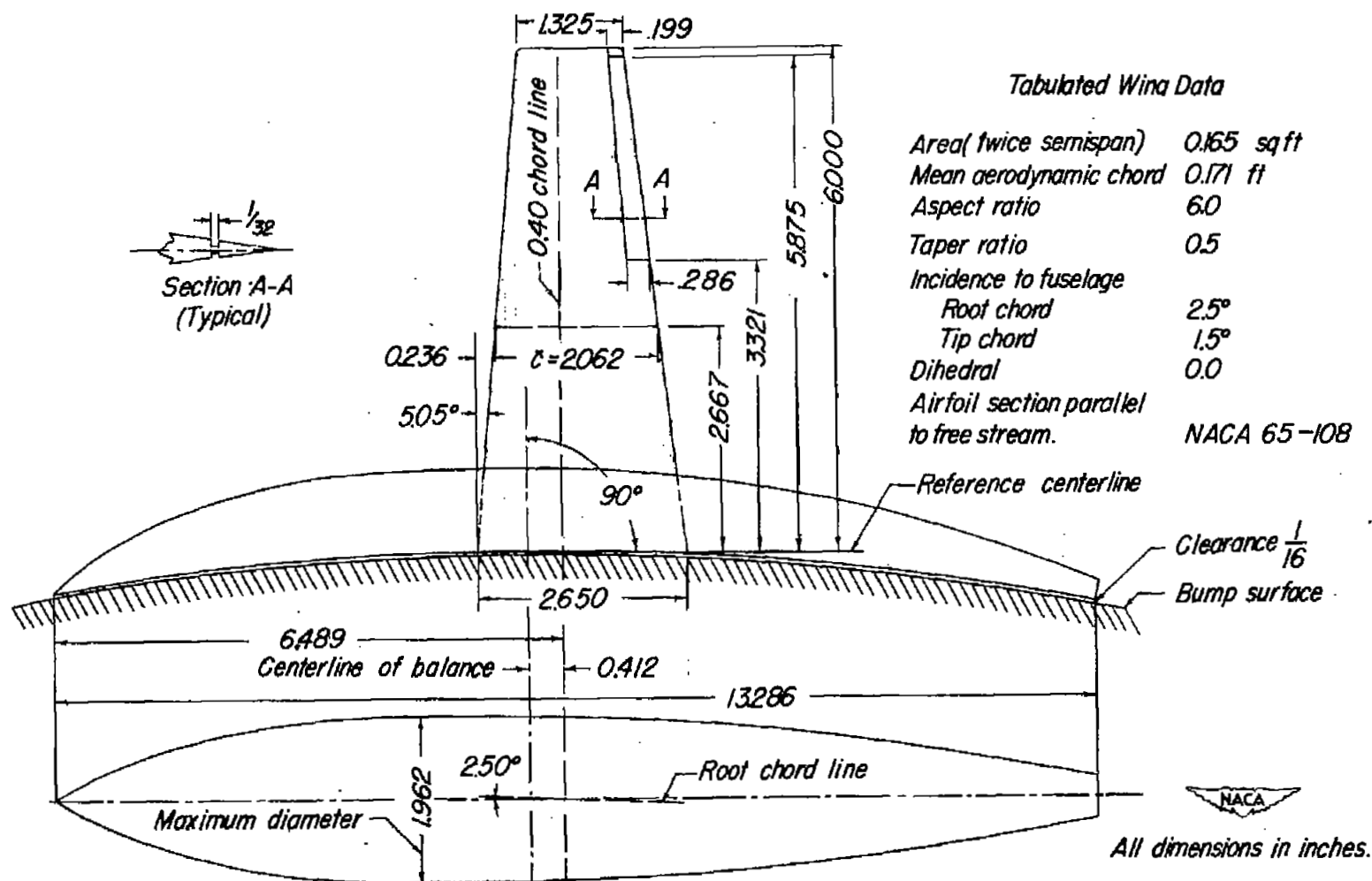


Figure 1.- General arrangement of $\frac{1}{28}$ -scale model of the X-1 airplane wing-fuselage combination.

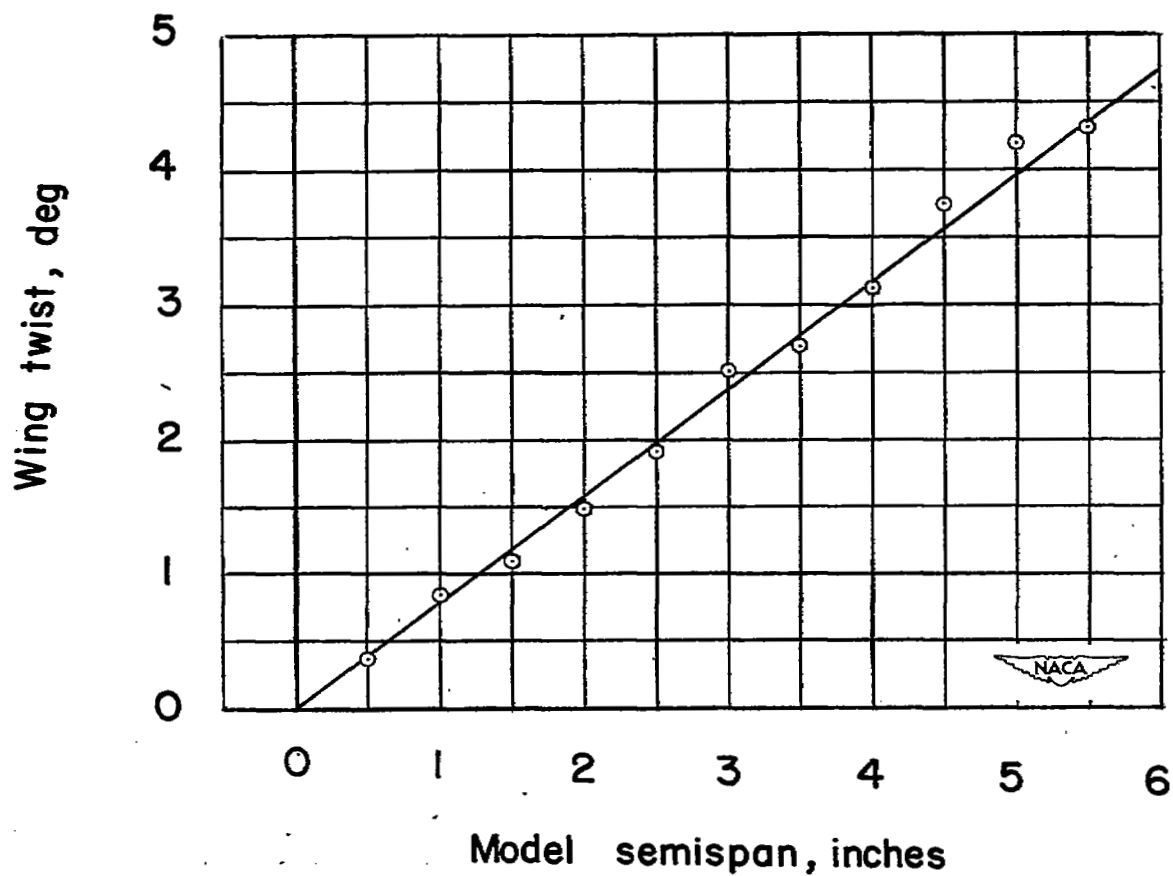


Figure 2.- Additional twist of damping-in-roll model.

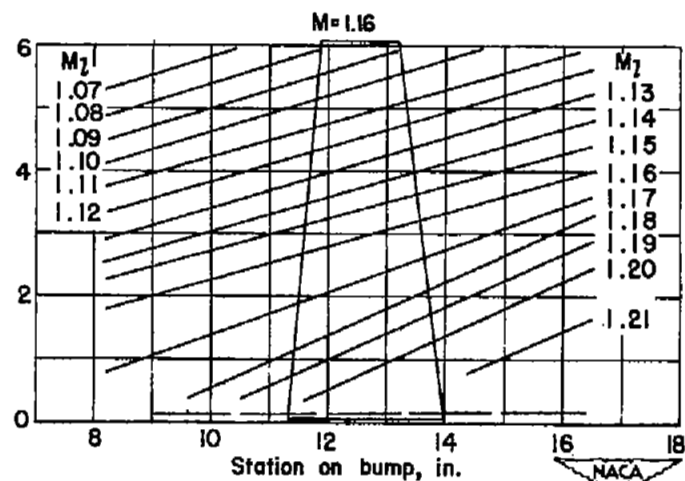
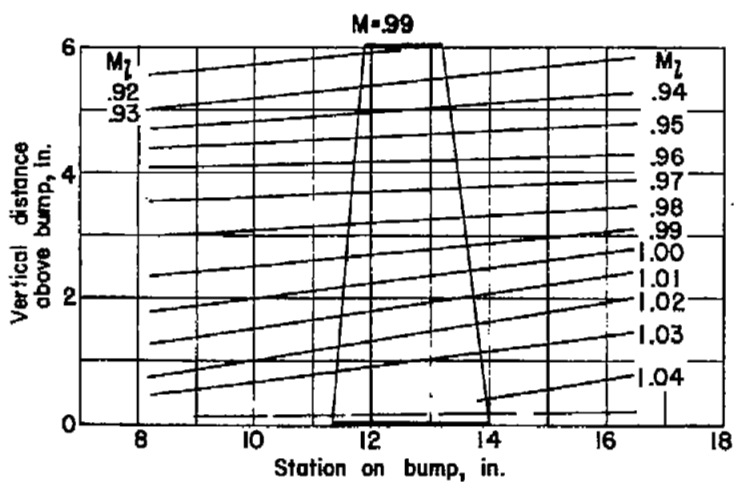
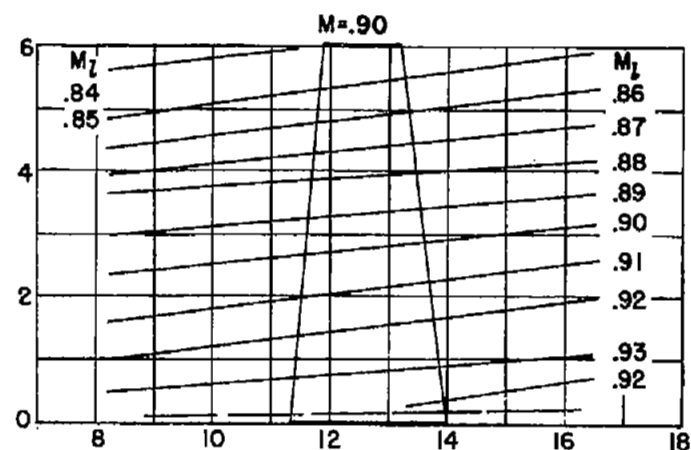
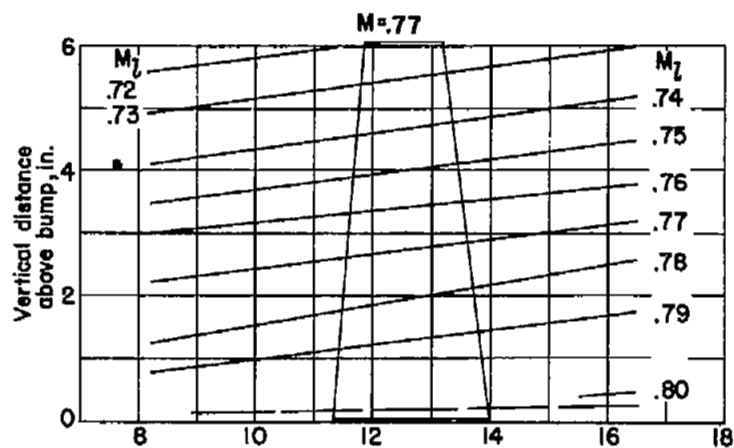


Figure 3.- Typical Mach number contours over transonic bump in region of model location.

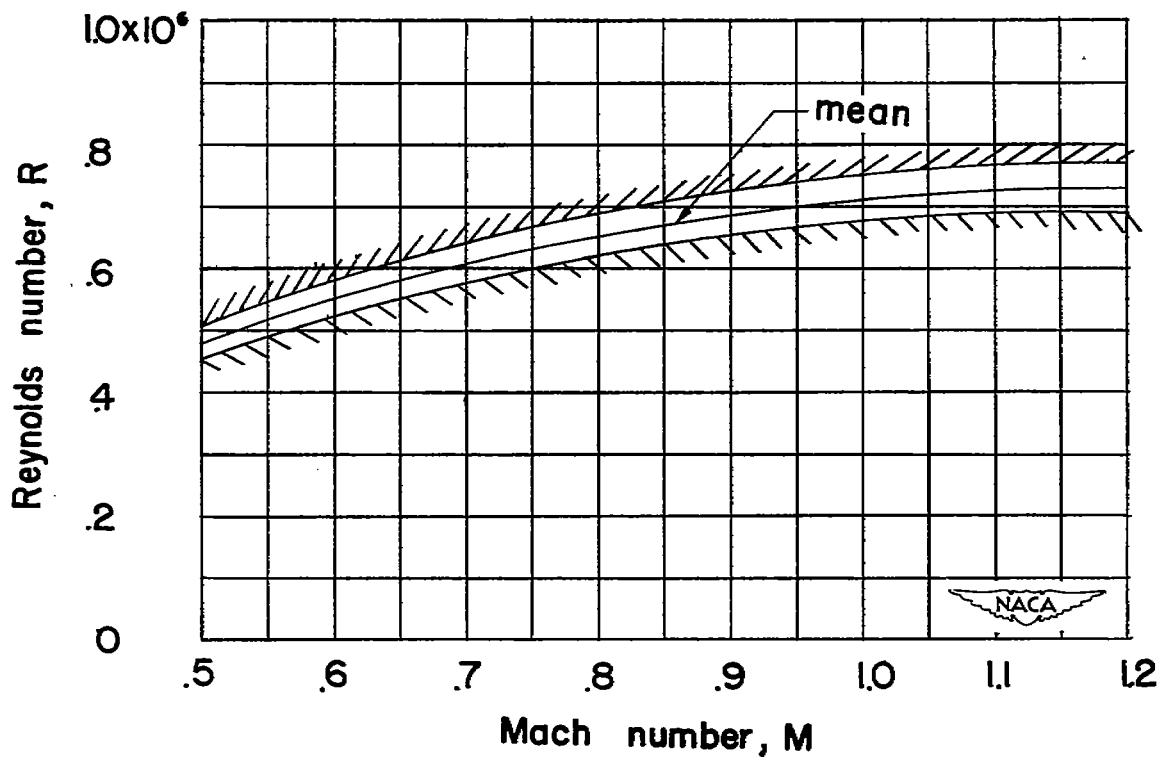


Figure 4.- Variation of Reynolds number with test Mach number through the transonic speed range.

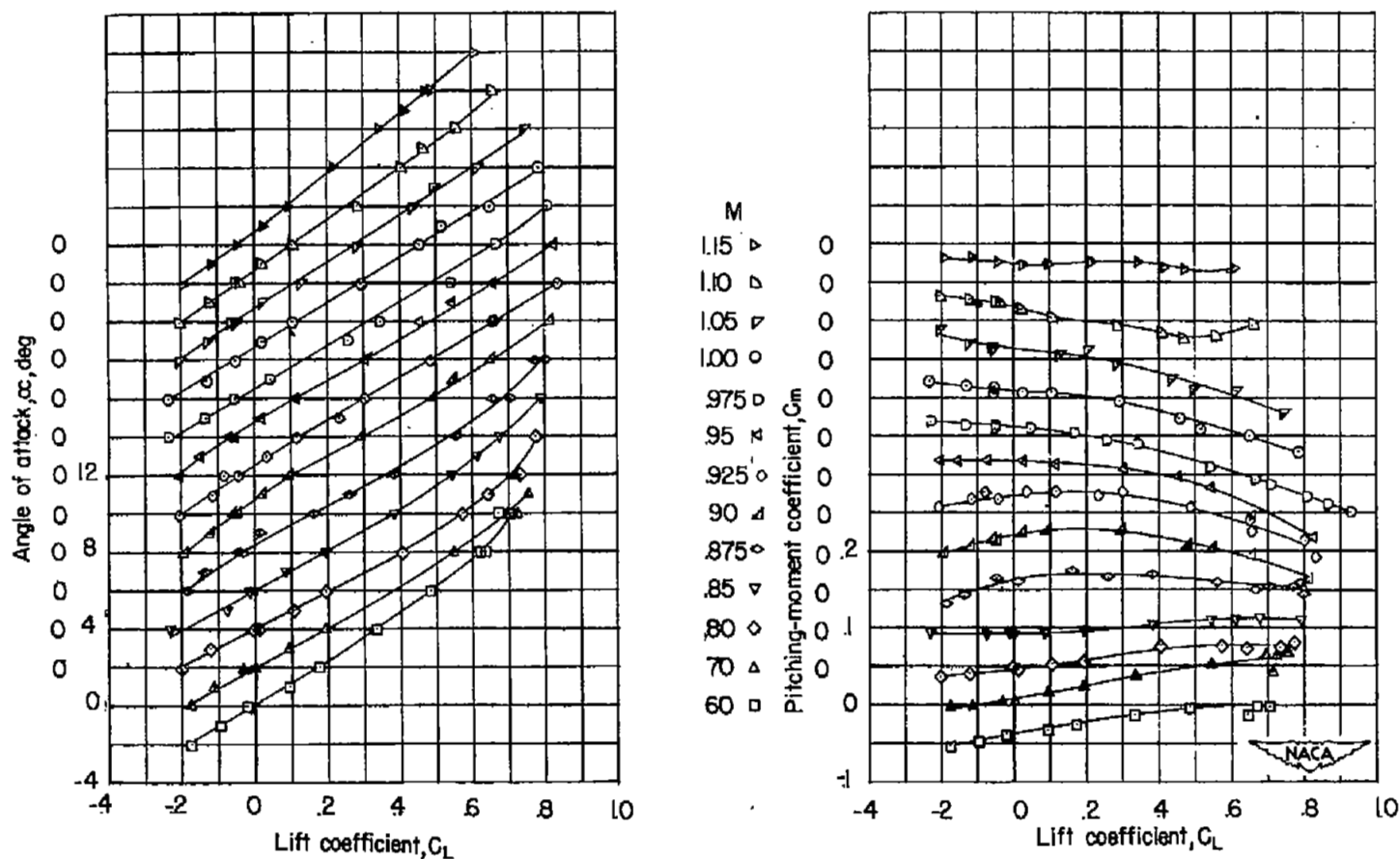


Figure 5.- Aerodynamic characteristics of a $\frac{1}{28}$ -scale model of the X-1 airplane wing-fuselage combination.

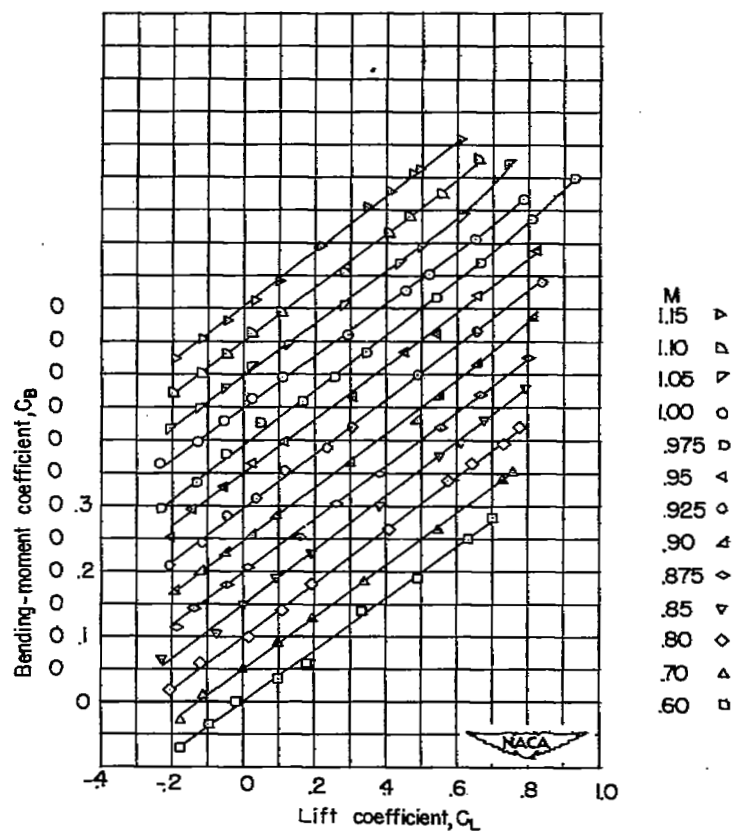


Figure 5.- Concluded.

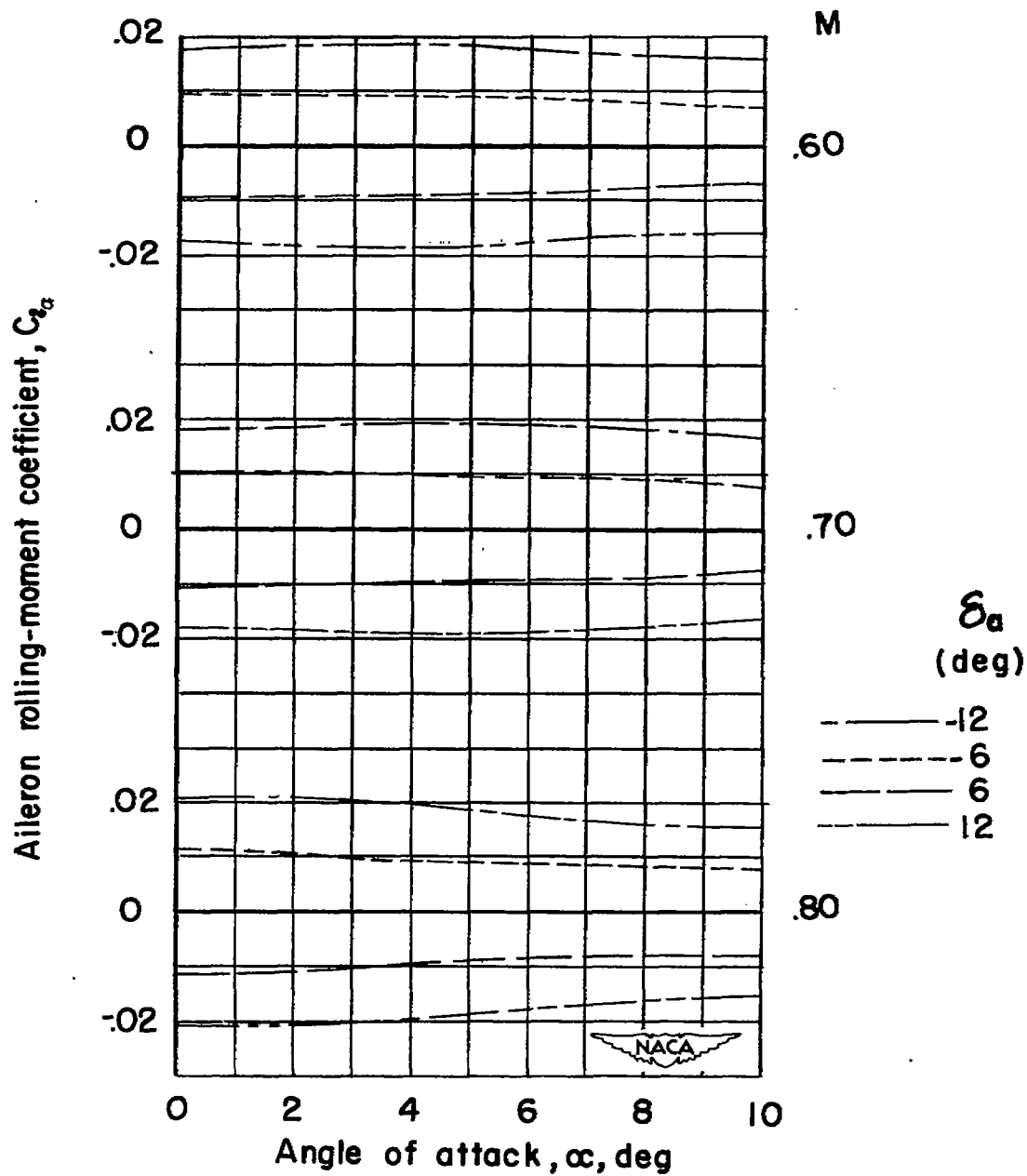


Figure 6.- Variation of aileron effectiveness with angle of attack and Mach number.

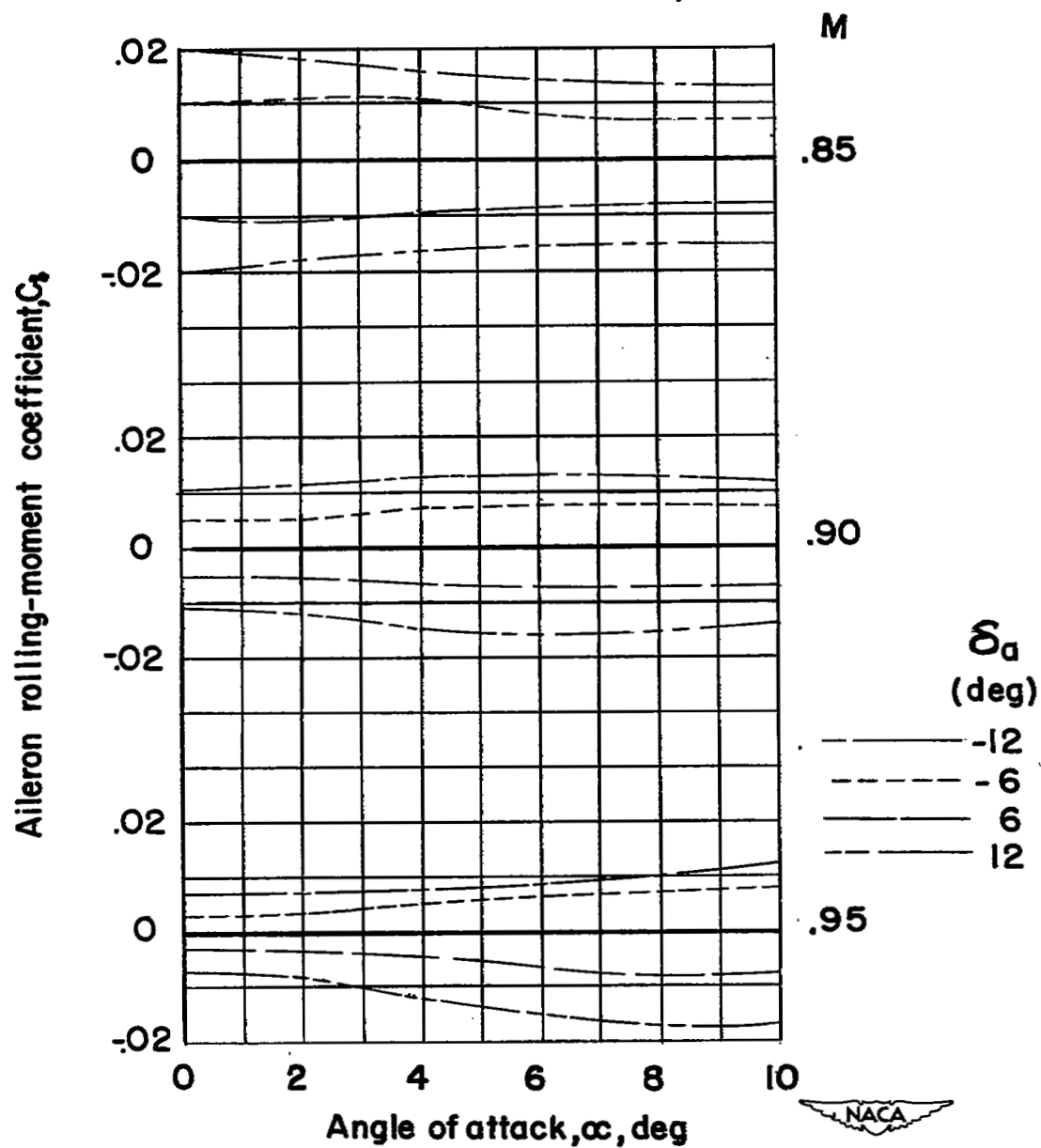


Figure 6.- Continued.

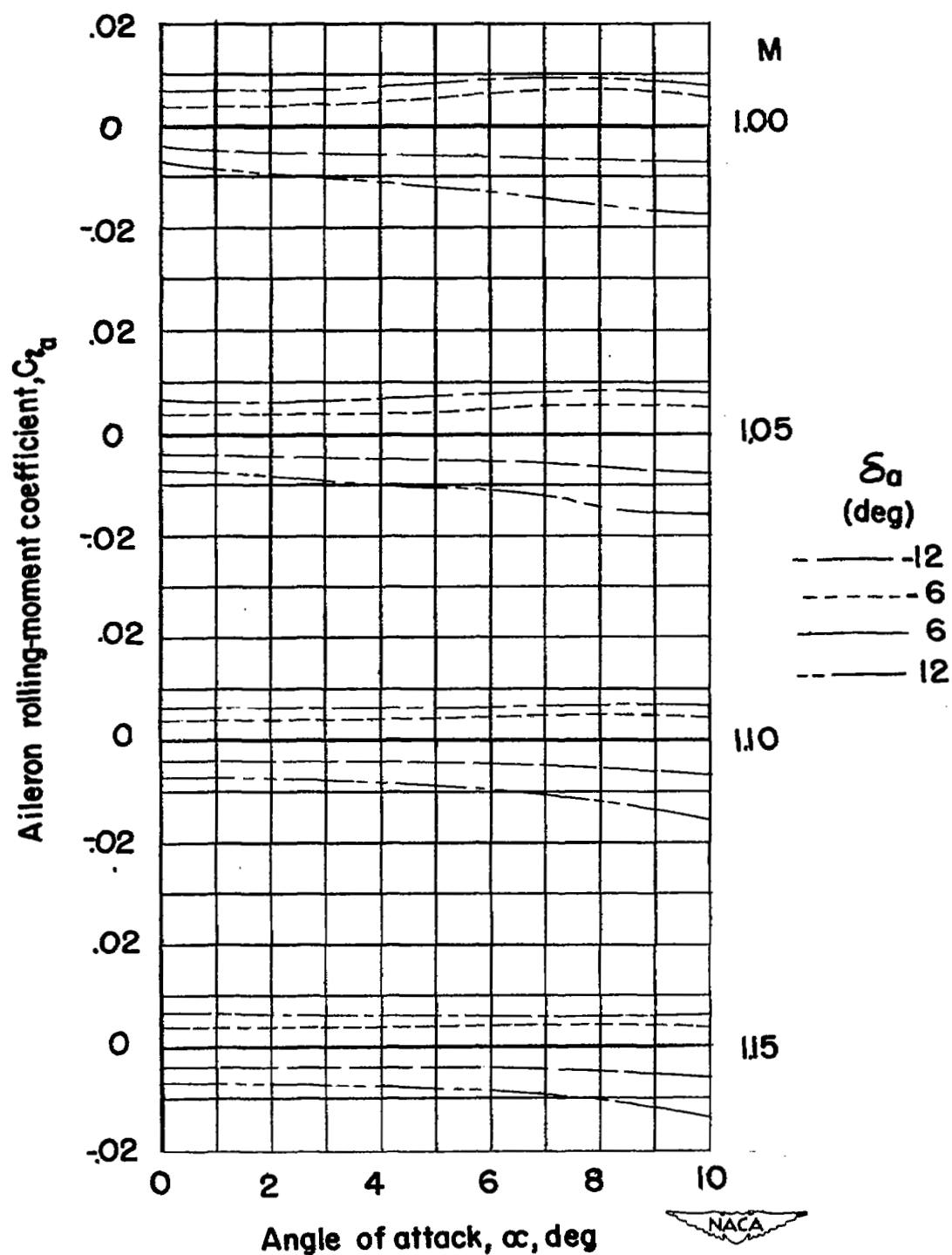


Figure 6.- Concluded.

~~CONFIDENTIAL~~

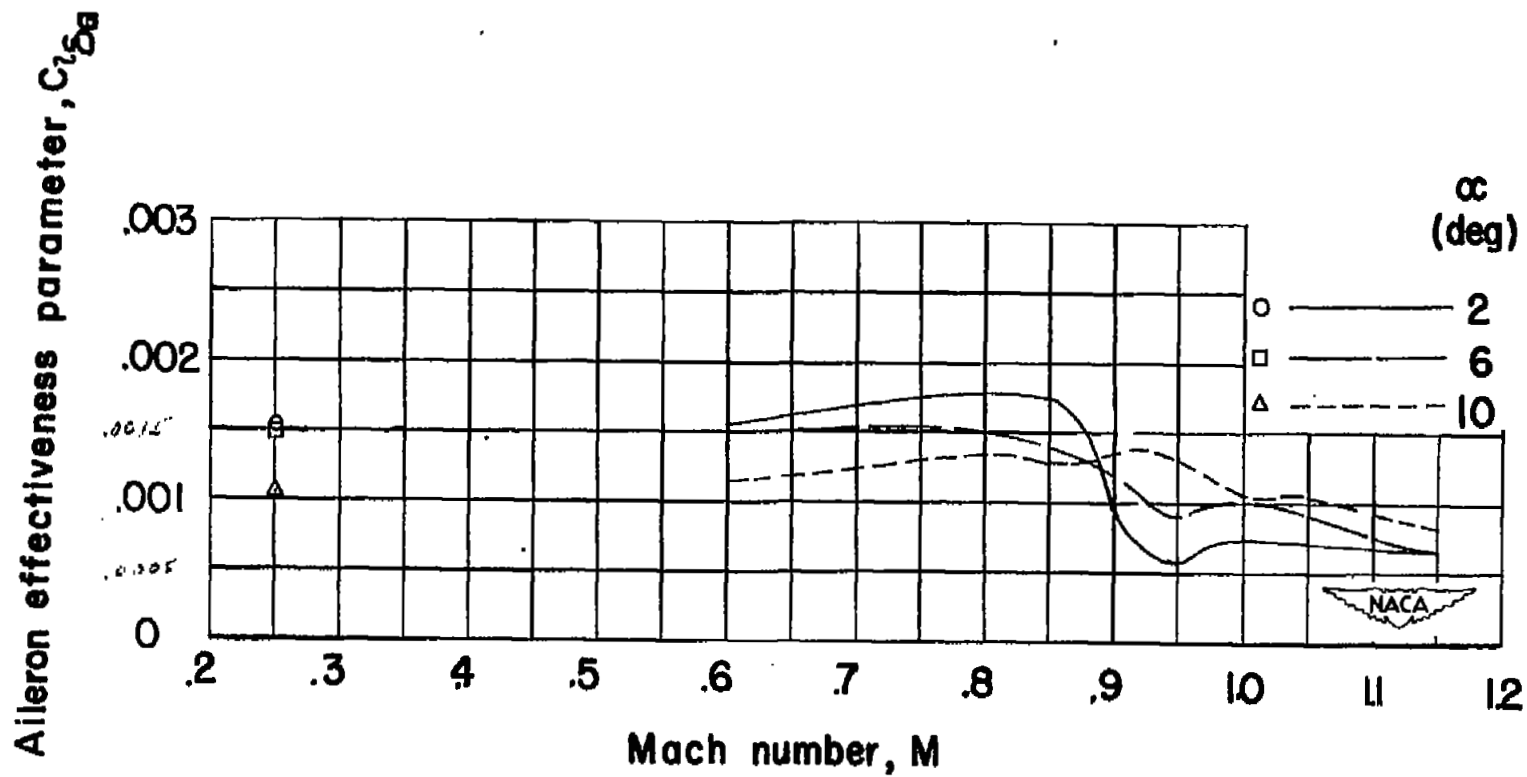


Figure 7.- Effect of Mach number and angle of attack on the aileron effectiveness.

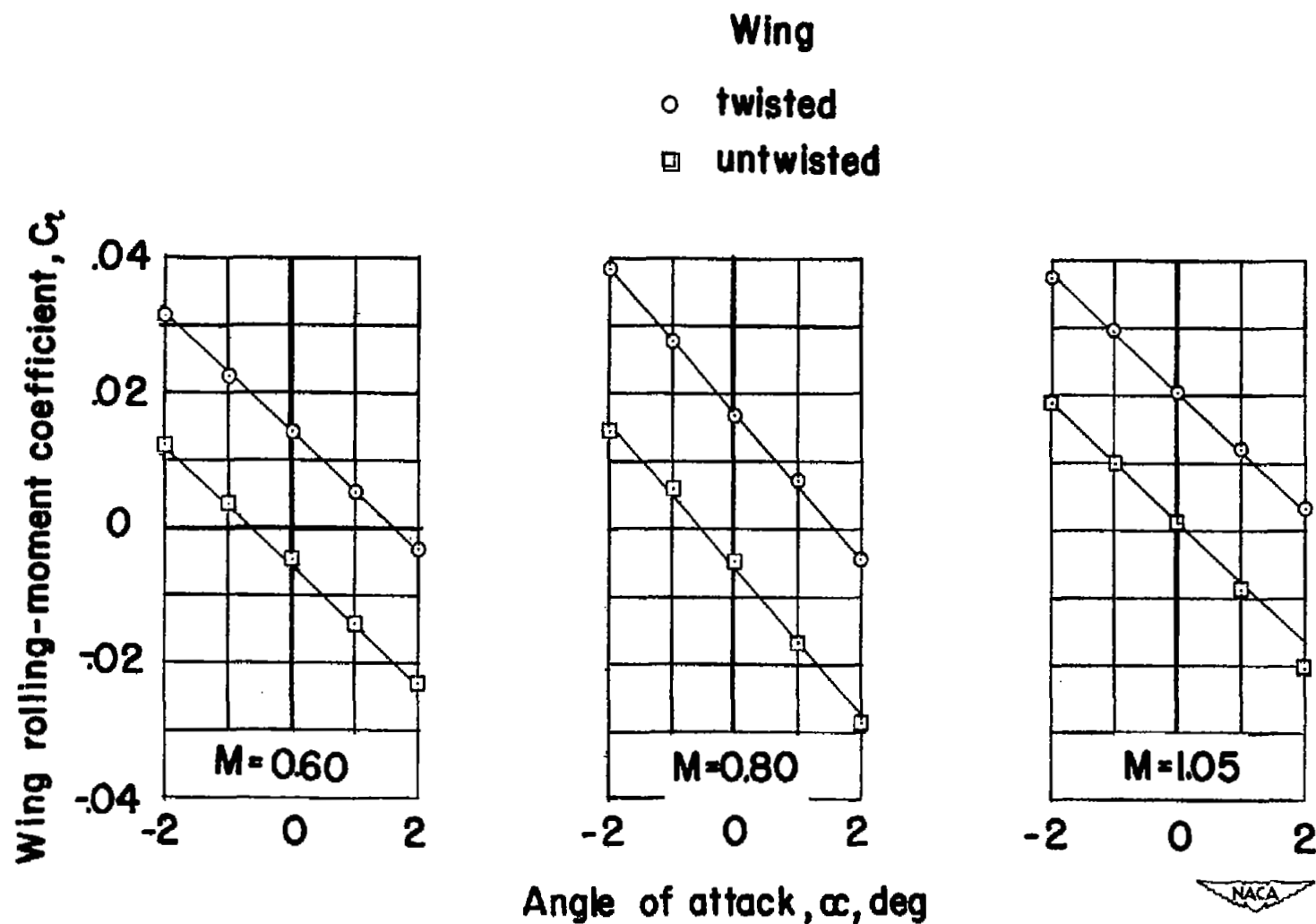


Figure 8.- Typical variation of wing rolling-moment coefficient with angle of attack for the twisted and untwisted wings.

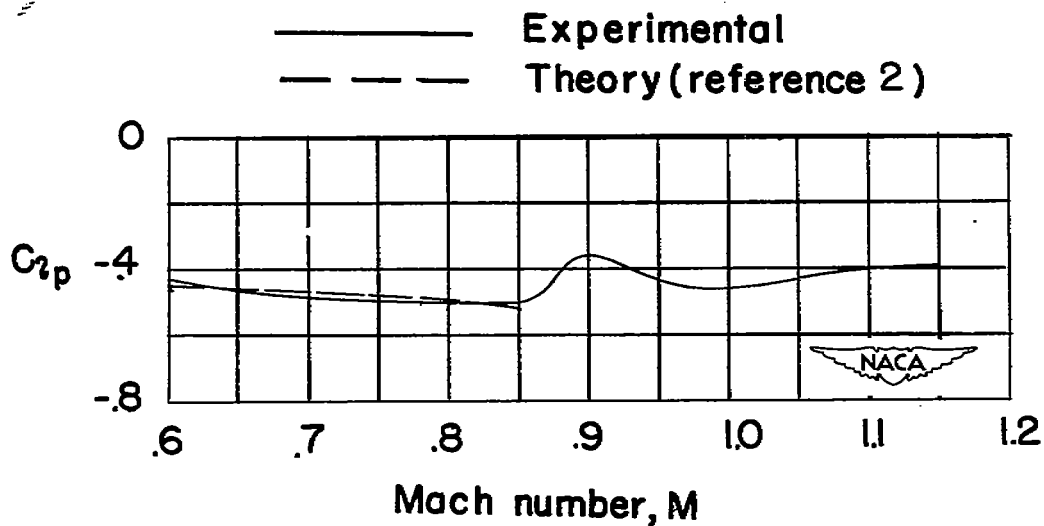


Figure 9.- Variation of damping-in-roll coefficient with Mach number as determined from tests of a twisted wing.

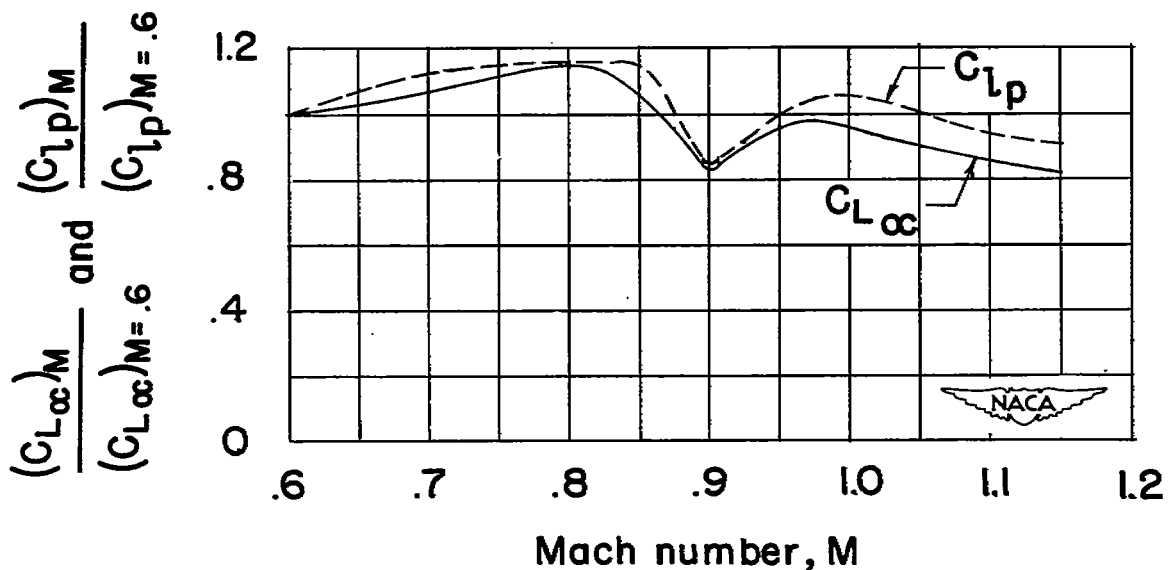


Figure 10.- Ratios of $(C_{l_{\alpha}})_M$ to $(C_{l_{\alpha}})_{M=0.6}$ and $(C_{lp})_M$ to $(C_{lp})_{M=0.6}$.

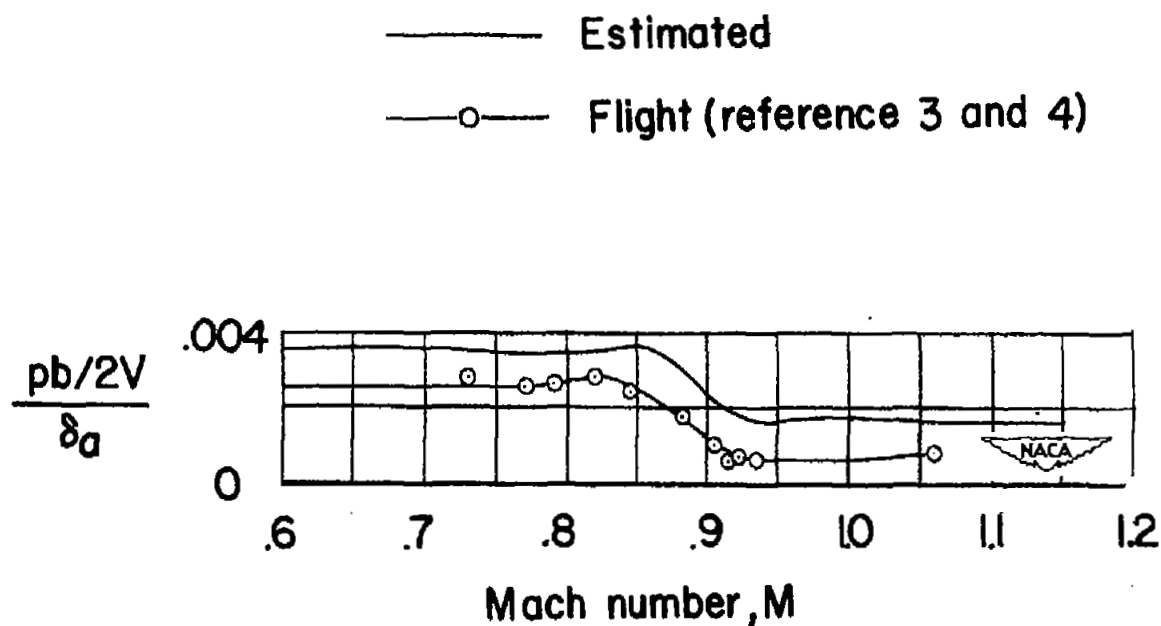


Figure 11.- Comparison of estimated values of $\frac{pb/2V}{\delta_a}$ with those obtained from flight tests at $C_L = 0.23$.

Scale	Tunnel	Airfoil thickness	Ref
—	1/28 bump	.08	
○	1/4 7by10	.10	unpublished
- - -	1/40 bump	.08	unpublished
—	theory	.08	2

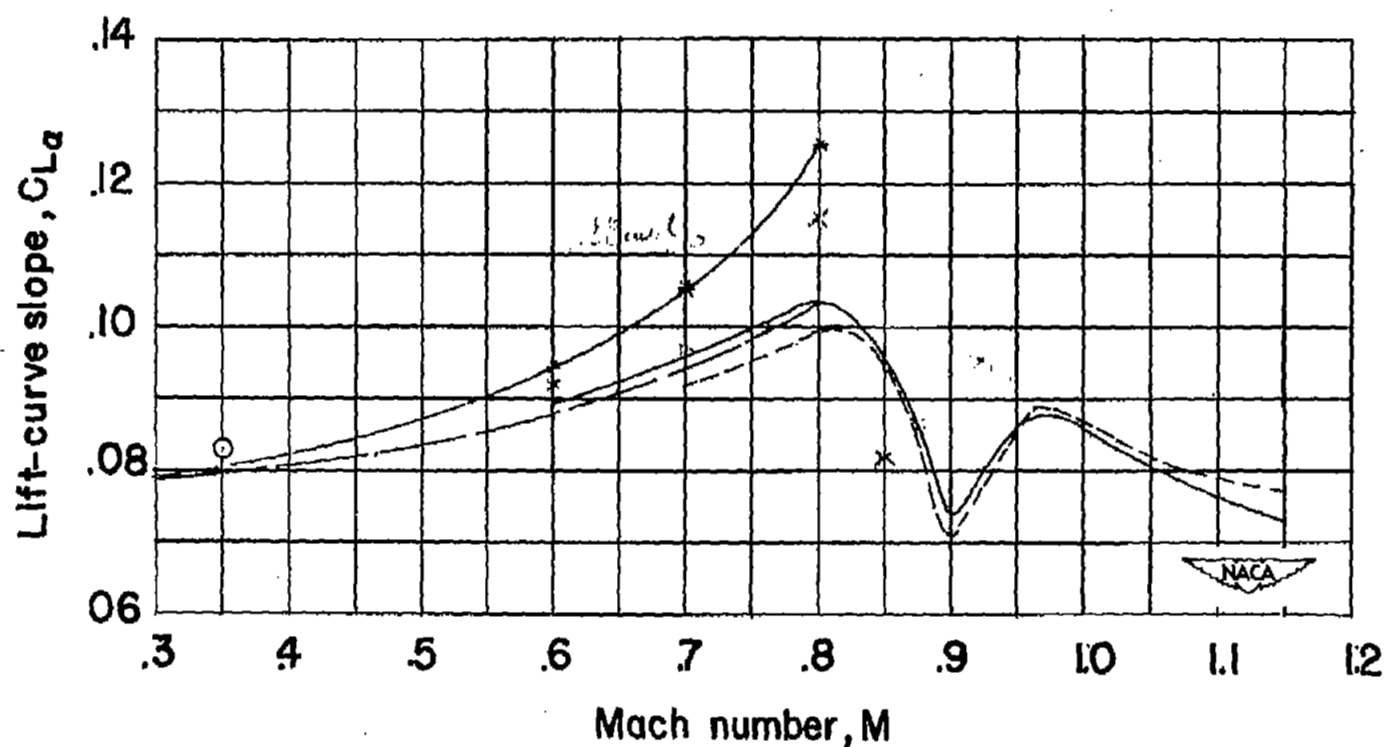


Figure 12.- Comparison of lift-curve slopes.

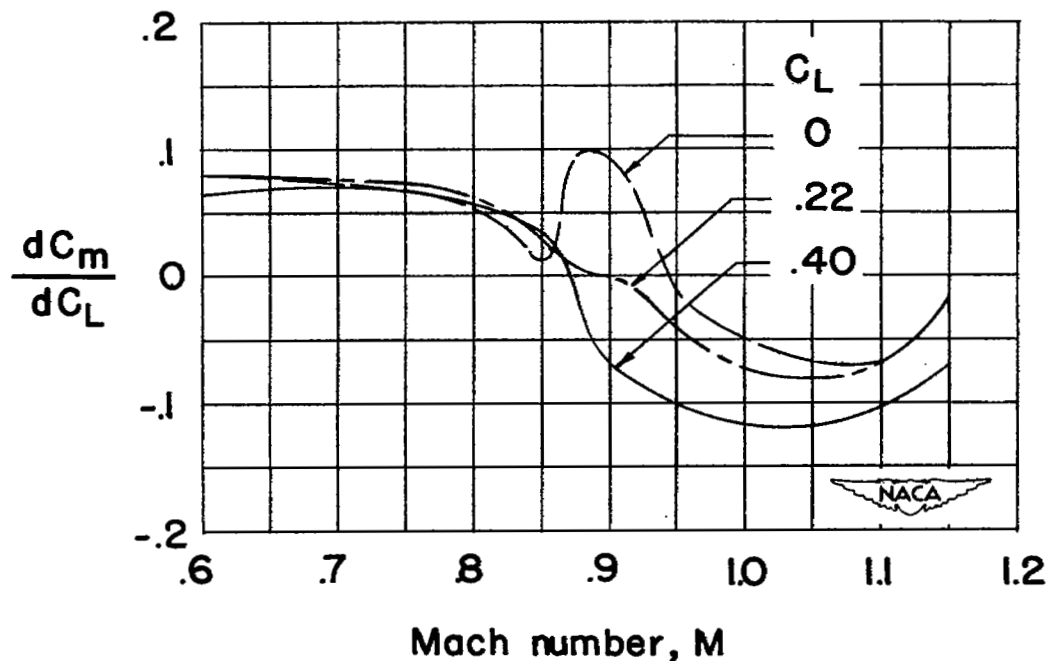


Figure 13.- Effect of lift on dC_m/dC_L for the model wing-fuselage combination. Center of gravity at 0.25 mean aerodynamic chord.

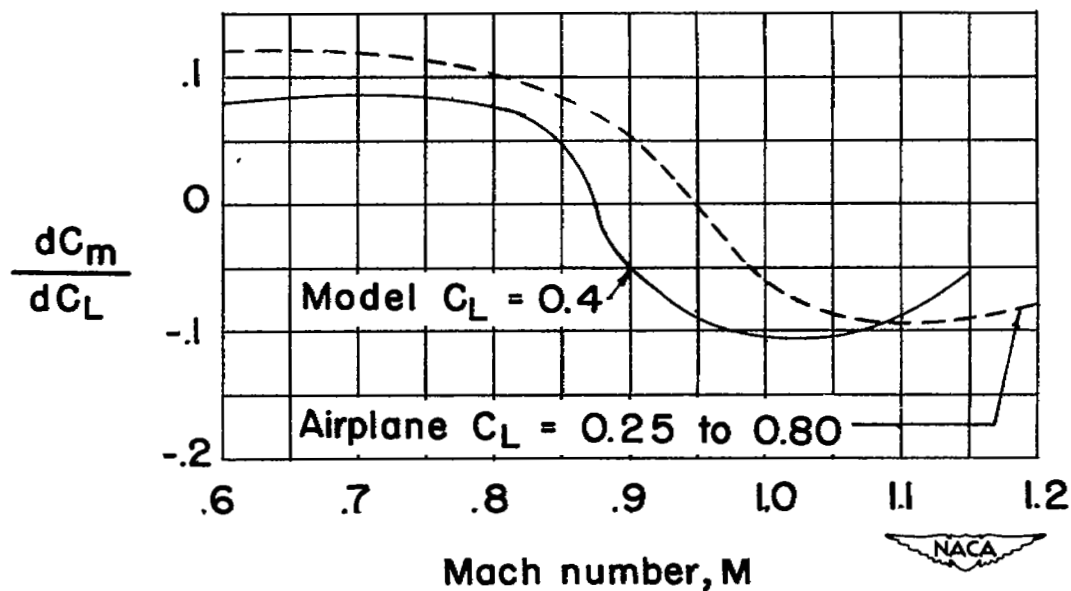


Figure 14.- Comparison of dC_m/dC_L obtained between model and airplane. Center of gravity at 0.236 mean aerodynamic chord.

~~CONFIDENTIAL~~

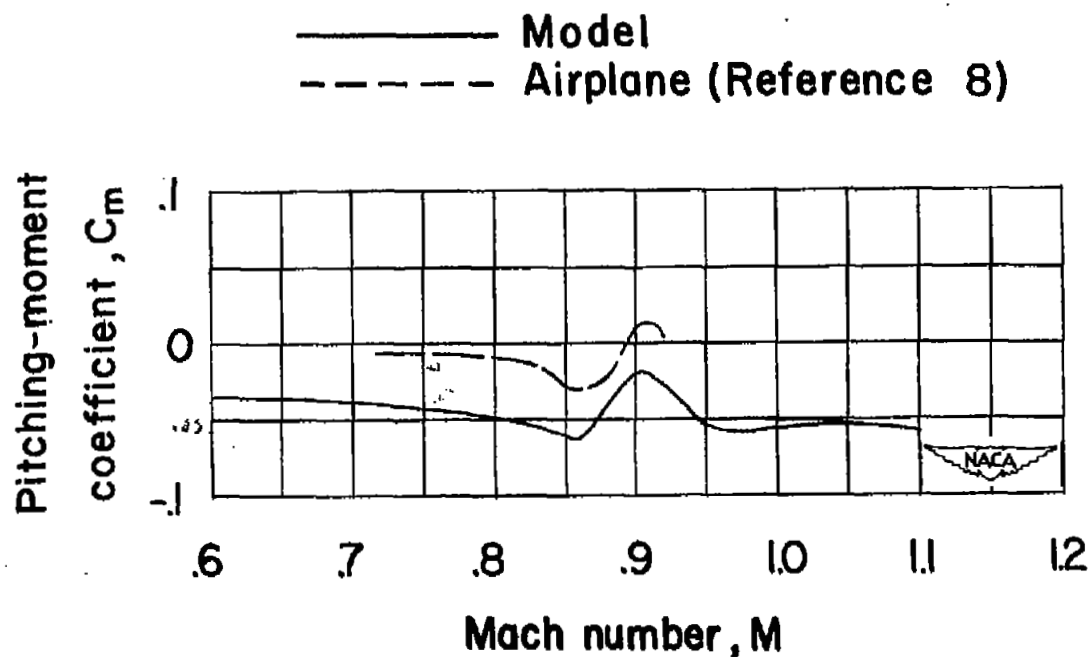


Figure 15.- Variation of pitching-moment coefficient with Mach number for the wing-fuselage combination at $C_L = 0.22$.

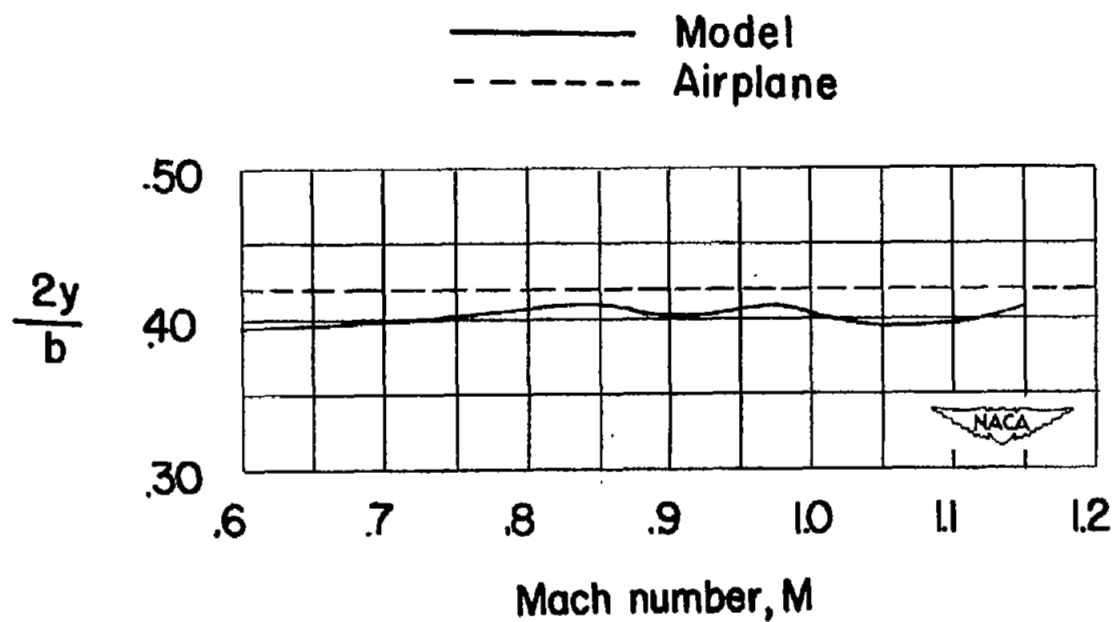


Figure 16.- Variation of lateral center of pressure of wing-fuselage combination with Mach number.